International Journal of Technology 14(1) 119-128 (2023)
Received May 2022 / Revised July 2022 / Accepted August 2022

International Journal of Technology

http://ijtech.eng.ui.ac.id

Utilization of $BaAl_{1.4}Si_{0.6}O_{3.4}N_{0.6}:Eu^{2+}$ Green-emitting Phosphor to Improve Luminous Intensity and Color Adequacy of White Light-emitting Diodes

Nguyen Le Thai[1], Thuc Minh Bui[2], Anh Tuan Le[3*], Dieu An Nguyen Thi[4]

[1]*Faculty of Engineering and Technology, Nguyen Tat Thanh University, Ho Chi Minh City, Vietnam*
[2]*Faculty of Electrical and Electronics Engineering, Nha Trang University, Nha Trang City, Vietnam*
[3]*Faculty of Electrical and Electronics Engineering, Ton Duc Thang University, Ho Chi Minh City, Vietnam*
[4]*Faculty of Electrical Engineering Technology, Industrial University of Ho Chi Minh City, Ho Chi Minh City, Vietnam*

Abstract. $BaAl_{1.4}Si_{0.6}O_{3.4}N_{0.6}:Eu^{2+}$ exhibiting broad excitation and emission bands with intense green emission centred at 510 nm is applied to produce high-performance white-light-emitting diodes (WLEDs). The preparation of the green phosphor utilizes $NaNO_3$ molten salt to attain the purity phase and enhanced luminescence strength boosting the crystalline growth. The influences of $BaAl_{1.4}Si_{0.6}O_{3.4}N_{0.6}:Eu^{2+}$ on the lighting intensity and color adequacy are investigated at three correlated color temperatures (CCTs) of 3000 K, 4000 K and 5000 K. The lighting output of the WLEDs with high CCTs (4000 – 5000 K) is deemed as enhanced with increasing green-phosphor concentration. The lower CCT shows greater lumen output when using a lower concentration of $BaAl_{1.4}Si_{0.6}O_{3.4}N_{0.6}:Eu^{2+}$. This tendency also takes place in the case of color uniformity. Conversely, the high concentration of the phosphor is not favourable to the color rendition property of the WLED because of the excessive green-light proportion. It is recommended to keep the concentration of $BaAl_{1.4}Si_{0.6}O_{3.4}N_{0.6}:Eu^{2+}$ staying below 10 wt% for better color fidelity.

Keywords: $BaAl_{1.4}Si_{0.6}O_{3.4}N_{0.6}:Eu^{2+}$; Color adequacy; Color rendering index; Color quality scale; Luminous intensity; White light-emitting diodes

1. Introduction

WLEDs have been recognized as a crucial and potential source for modern-day illumination applications, such as household lighting, display devices, microprocessors, and multiplexers (Karadza, *et al.,* 2022; Zhong *et al.,* 2019). Hence, the development of WLED structure yielding higher effectiveness to meet certain optical requirements for certain application field is always critical. One of the most common types of WLEDs is the phosphor-converting WLED, in which the phosphor acts as an agent to convert the emitted light from the near-UV or blue LED chips. The YAG:Ce^{3+} phosphor with great yellow emission is widely utilized for traditional LED (Zhou *et al.,* 2020; Chen *et al.,* 2019). The luminescence of the WLED using Ce^{3+}-doped YAG is excellent, with a significant quantum efficiency (about 90%), thus, it is suitable for high-intensity LED. Unfortunately, the color rendering of this phosphor is not impressive, which limits the growth of WLED in fields

*Corresponding author's email: leanhtuan1@tdtu.edu.vn, Tel.: +84-09-34001680, Fax. +84-09-34001680
doi: 10.14716/ijtech.v14i1.5666

that require high color reproduction performance (Su and Gao, 2020; Nahavandi et al., 2020). Therefore, introducing good phosphor materials for high luminous intensity with sufficient chromatic rendition has been the objectives for researchers. It is reported that these mentioned issues could be addressed by getting the blue, green and red phosphor excited under the near UV LED to compensate for the lack of green and red spectra which exists in the case of using only YAG:Ce^{3+} (Wang *et al.,* 2021; Anh, Le, and Lee, 2019). The green phosphor might be a good choice for attaining good CCT consistency and high luminous intensity of WLEDs (Keshri *et al.,* 2020; Hao *et al.,* 2019).

The rare earth ions with broadband emission (Eu^{2+} and Ce^{3+}) are good for obtaining excellent quantum efficacy with great thermal stability. This can be ascribed to their broad emission spectrum that could cover the near-UV and blue wavelength critical for achieving good chromatic rendering ability and short decay time that could prevent saturation effects. Choosing suitable host compositions for them to magnify their advantages. The oxynitride/nitride phosphor is extensively investigated as the host compound for this type of rare-earth dopant since it provides high chemical and thermal stability. The luminescence of europium-doped (oxy)nitride phosphor is reported to have significant strength. For instance, the intense emission color of green can be recorded in the cases of β-sialon:Eu^{2+} and $MSi_2O_2N_2:Eu^{2+}$ (M = Ca, Sr, Ba) (Xu *et al.,* 2021; David, Sahlhoff, and Wisser, 2019). $M_2Si_5N_8$ (M = Ca, Sr, Ba) and $MAlSiN_3$ (M = Ca or Sr) exhibited peak emission of about 600 nm or event at broader band of wavelengths (Ji *et al.,* 2020; Wang *et al.,* 2019).

This paper therefore utilizes the europium-doped (oxy)nitride phosphor to develop the WLED configuration. The WLED model uses the green phosphor of $BaAl_{1.4}Si_{0.6}O_{3.4}N_{0.6}:Eu^{2+}$ as the additional phosphor material, besides the original YAG: Ce^{3+}, to stimulate the scattering effects, reducing the energy loss by light trapped and backward scattering, which is essential for high chromaticity and luminescence of a WLED. The WLEDs are simulated with three preset CCTs: 3000 K, 4000 K, and 5000 K. The concentration of phosphor is modified between 5 and 10 wt%. The phosphor is prepared via molten salt synthesis to accomplish a desirable purity phase and crystal growth. The finding shows that the phosphor is a good choice for high-luminescence WLEDs that need adequate color rendering properties.

2. Phosphor Preparation and Characterization

2.1. Preparation of $BaAl_{1.4}Si_{0.6}O_{3.4}N_{0.6}:Eu^{2+}$

The molten salt $NaNO_3$ is used for the preparation of the $BaAl_{1.4}Si_{0.6}O_{3.4}N_{0.6}:Eu^{2+}$ with 5% mol of Eu-doping concentration. The purpose of using $NaNO_3$ is to attain the purity of the phosphor sample as this salt is easily melted at relatively low temperatures and plays a role as a high-temperature solvent to enhance the efficiency of reactants' diffusion (Ma *et al.,* 2021). The phosphor composition includes $BaCO_3$, Al_2O_3, Eu_2O_3, α-Si_3N_4, and $NaNO_3$. The phosphor synthesis is started with grinding $BaCO_3$, Al_2O_3, and Eu_2O_3 and followingly going through a 3-hour calcination process at 1450°C. Then, the product is cooled down to room temperature. $NaNO_3$ and α-Si_3N_4 are then mixed with the attained powder, and the compound is re-ground for an hour. Subsequently, it is burned for 6h at 1300°C in the reducing atmospheric condition of N_2/H_2 (8:1). Note that the mass ratio of the raw ingredients and the molten salt $NaNO_3$ is 1:2. After the heating stage, the powder stays in the furnace and is cooled down to room temperature before being was with deionized water to get rid of the residues. After that, it is put into a drying oven and heated at 80°C for 5h (Xi *et al.,* 2021; Elkarim *et al.,* 2021).

The prepared phosphor performs uniform-dispersed morphology with a standard spherical shape while demonstrating high crystallization and dispersibility. This is because

the $NaNO_3$ liquid solvent creates an absorbing layer on the formed crystalline, preventing the aggregation phenomenon by penetrating ions Na^+. Besides, the liquid environment provided by the $NaNO_3$ molten salt is beneficial to the crystal growth, contributing to forming the spherical shape for the synthesized phosphor $BaAl_{1.4}Si_{0.6}O_{3.4}N_{0.6}:Eu^{2+}$. Furthermore, this enhancement in crystalline formation is more beneficial to the luminous efficacy of the phosphor material (Li *et al.,* 2021; Zhang *et al.,* 2020).

2.2. $BaAl_{1.4}Si_{0.6}O_{3.4}N_{0.6}:Eu^{2+}$ photoluminescence analysis

The synthesized phosphor $BaAl_{1.4}Si_{0.6}O_{3.4}N_{0.6}:Eu^{2+}$ exhibits the broad excitation region of UV-to-blue wavelength. Its strong green emission spectrum is recognized in the wide range of 460 nm – 600 nm, peaking at 510 nm. This could be attributed to the transitions of Eu^{2+} ion from $4f^65d^1$ to $4f^7$. Besides, the intensity of phosphor luminescence is affected by the molten salt addition. The luminous intensity could be enhanced with the increasing amount of $NaNO_3$, yet the following decrease can be recognized since the excessive liquid phase medium causes the incomplete reaction leading to the probability of impurity and surface defects for the phosphor particles. With the applied mass ratio of 1:2 for raw materials – $NaNO_3$, the intensities under 365 nm and 450 nm excitation bands are heightened by 17% and 13%, respectively.

Besides, the emission intensity's increase and subsequent decrease is also caused by the concentration quenching when doping Eu^{2+}. The concentration quenching influences could be examined with the distance between the doped ions in the host lattice, also known as the energy-transfer critical distance (R_C) (Quesnel *et al.,* 2021; Yang *et al.,* 2021). This R_C can be expressed as the following computation:

$$R_C = 2\left[\frac{3V}{4\pi x_c Z}\right]^{1/3} \quad (1)$$

x_c is the critical doping concentration of Eu^{2+} in the phosphor composition, Z and V are the amount of Eu^{2+}-substituted cations within the unit cell and the unit-cell volume, respectively. In this work, V and Z are determined to be 831.19 Å and 8, respectively. while the x_c of the ion Eu^{2+} is equal to 0.05. As a result, the computed R_C is 15.84 Å. Generally, the R_C is smaller than 4 Å, but in the case of green phosphor, a larger R_C is determined, indicating that the energy transfer among the ions Eu^{2+} does not mainly take place by the exchange interaction. Consequently, the multipolar interaction might be responsible for the mechanism of Eu^{2+} energy transfer, which could be calculated based on the theory of Dexter (Le *et al.,* 2021; Zhu *et al.,* 2019):

$$\frac{I}{x} = k\left[1 + \beta(x)^{Q/3}\right]^{-1} \quad (2)$$

x, k and β is the doping concentration of Eu^{2+} are the doping concentration of Eu^{2+}, and constants under the same source of excitation for the given host, respectively. I is the emission intensity, and $\frac{I}{x}$ indicates the emission strength per Eu^{2+} concentration. Q shows the multipolar interactions' constraints. Note that Q = 6, 8, 10 corresponding to the interactions of dipole-dipole, dipole-quadrupole, or quadrupole-quadrupole. Accordingly, computed Q is about 5.79, nearly 6, meaning that the multipolar interaction that controls the electron transfer mechanism and the effect of Eu^{2+}-doping concentration quenching is the dipole-dipole.

The performance of the used phosphor is also influenced by thermal quenching. The thermal quenching of $BaAl_{1.4}Si_{0.6}O_{3.4}N_{0.6}:Eu^{2+}$ can be examined with the following formula:

$$I(T) = \frac{I_0}{1 + A\exp\left(\frac{-\Delta E}{k_B T}\right)} \quad (3)$$

I_0 indicates initial intensity, T is the given temperature at which the intensity I(T) can be determined. A is a pre-exponential factor and constant, k_B is a Boltzmann constant (El-Ghoroury *et al.,* 2020; Abeysekera *et al.,* 2020), and ΔE shows thermal-quenching activation energy which is determined as 0.2509 eV. The stability in thermal factor could be well performed by this $BaAl_{1.4}Si_{0.6}O_{3.4}N_{0.6}:Eu^{2+}$ with large activation energy for thermal quenching. In other words, the thermal quenching of the prepared green-emitting phosphor is small.

3. Results and Discussion

One of the critical factors to get the improvement in the color and luminescence performances of WLEDs is the reduction of the backscattering effect. The common approach is to enhance scattering efficiency to perform better light extraction and color blend. The concentration of the yellow phosphor $YAG:Ce^{3+}$ greatly affects this. Too high concentration or thicker film of $YAG:Ce^{3+}$ can induce significant thermal quenching that is disadvantageous to the light conversion but initiates the internal reflection loss. Thus, it may decrease color balance and light intensity. In other words, the emitted light tends to lean to the yellow region or becomes yellowish.

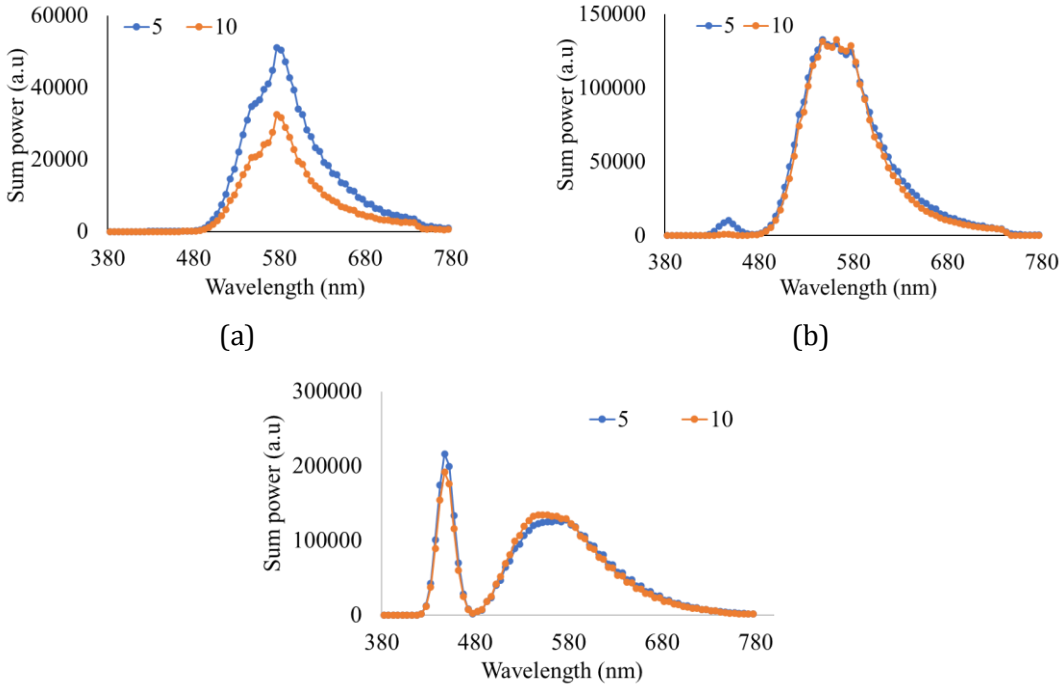

Figure 1 The emission spectra of WLEDs as a function of $BaAl_{1.4}Si_{0.6}O_{3.4}N_{0.6}:Eu^{2+}$ concentration at different CCTs: (a) 3000 K; (b) 4000 K; (c) 5000 K

The addition of green-emitting phosphor (GEP) $BaAl_{1.4}Si_{0.6}O_{3.4}N_{0.6}:Eu^{2+}$ performs significant changes in the concentration levels of YAG:Ce3+, which is presented in Figures 1. Regardless of the particle size and WLED's average CCTs, the reduction in the yellow phosphor concentration with the higher $BaAl_{1.4}Si_{0.6}O_{3.4}N_{0.6}:Eu^{2+}$ concentration is observed, regardless of the average CCTs. This phenomenon contributes greatly to the color-temperature stability, indicating noticeable benefits to the scattering and conversion effectiveness of the phosphor structure of the simulated WLED.

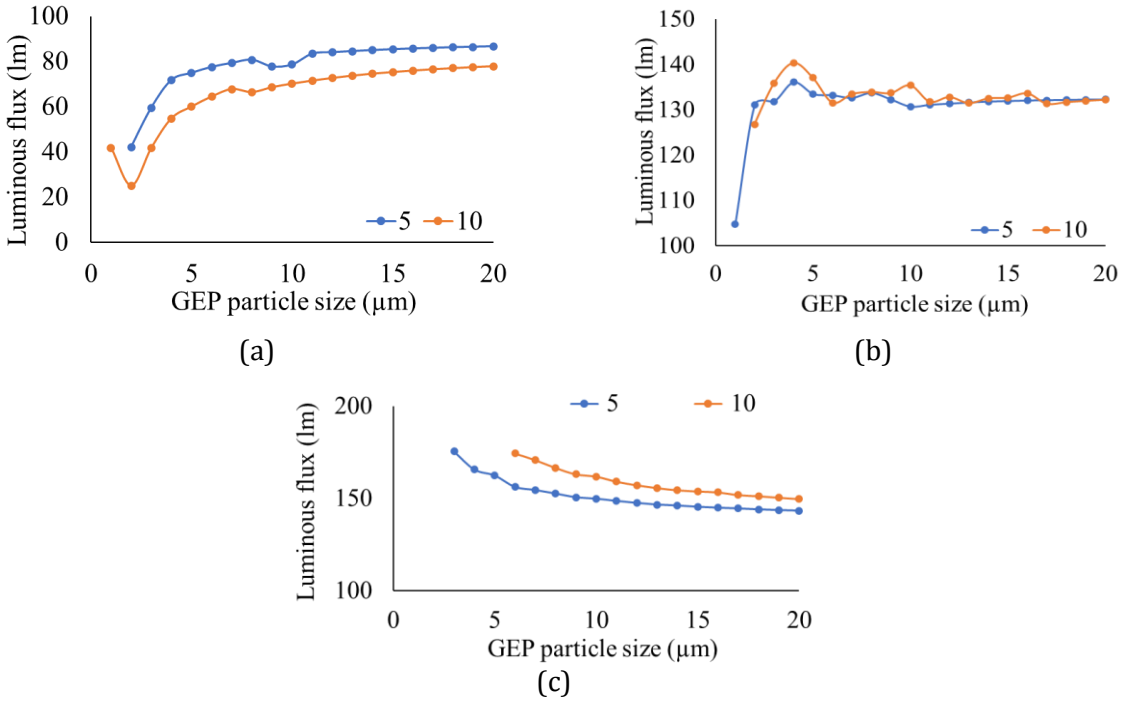

Figure 2 luminous flux of WLEDs as a function of $BaAl_{1.4}Si_{0.6}O_{3.4}N_{0.6}:Eu^{2+}$ concentration: (a) 3000 K; (b) 4000 K; (c) 5000 K

The emission power is also influenced by this change in phosphor concentrations, as depicted in Figures 2. Overall, GEP's presence helps to promote the intensity of green emission spectra. However, unlike the exhibited concentration of $YAG:Ce^{3+}$ in Figures 1, the performance of the WLED spectra depends on the monitored average CCTs. At a low CCT of 3000 K, a higher concentration of GEP brings lower performance, see Figures 2 (a). Meanwhile, 4000 K and 5000 K average CCTs, the difference between the two concentration levels of GEP is negligible. Nonetheless, the improvement in blue-light emission bands is recognized for the lower concentration (5 wt%) of $BaAl_{1.4}Si_{0.6}O_{3.4}N_{0.6}:Eu^{2+}$. Both blue (420 – 480 nm) and green (500 – 600 nm) bands are involved in forming white light. Consequently, their enhanced performance could induce the white-light generation efficacy. The higher emission lines in the blue wavelengths also expressed that the blue-light scattering and conversion are stimulated, which might be remarkably beneficial to the color uniformity of WLED.

The luminous flux (LF), which is expected to get benefits from the addition of the GEP $BaAl_{1.4}Si_{0.6}O_{3.4}N_{0.6}:Eu^{2+}$, is expressed in Figures 3. Since the sum power is CCT-dependent, the luminous flux is influenced not only by the concentration but also the CCT values. 3000-K WLED package presents higher LF with a smaller weight percentage of the GEP, which could be described by the emission spectra of the package shown in Figures 2 (a). Conversely, the stronger LF with the higher GEP concentration (10 wt%) is recorded in the 5000-K and 4000-K WLEDs. The increase of the LF in these two cases could be ascribed to the significant decrease of $YAG:Ce^{3+}$ with a greater amount of $BaAl_{1.4}Si_{0.6}O_{3.4}N_{0.6}:Eu^{2+}$ in the package. The lower the concentration of the yellow phosphor, the higher the probability of the light extracted from the LED and the lower the energy loss by reabsorption. This also marks an important use of $BaAl_{1.4}Si_{0.6}O_{3.4}N_{0.6}:Eu^{2+}$ for controlling the luminous flux of the WLED at high CCTs.

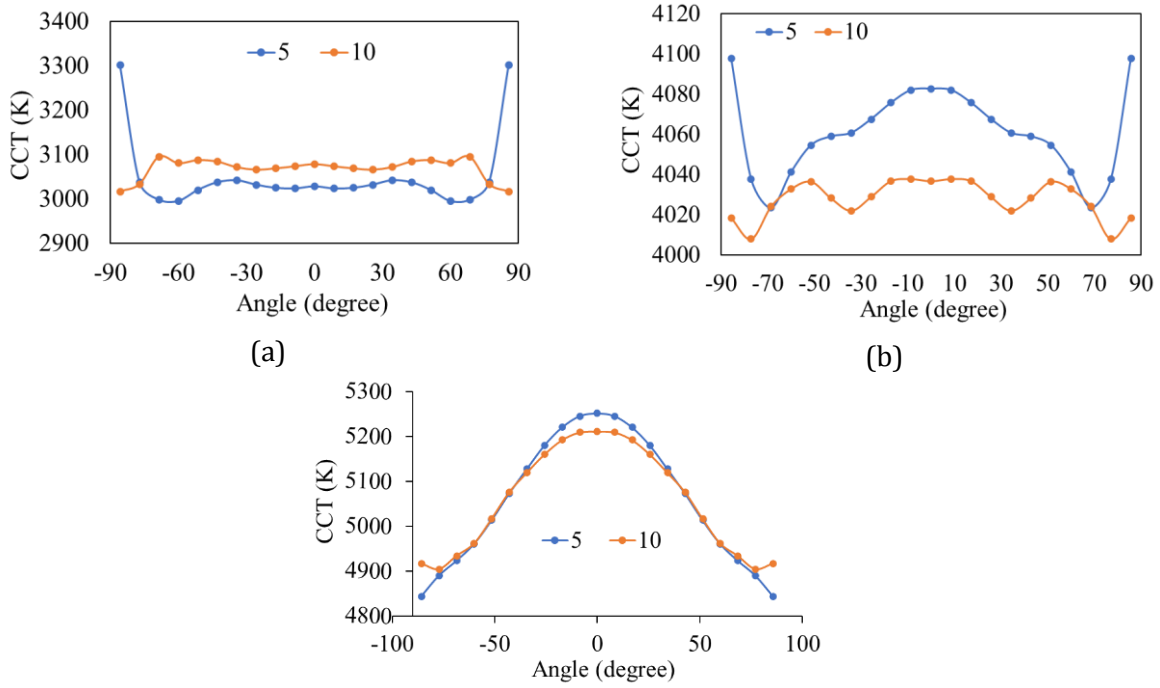

Figure 3 The CCT of WLEDs as a function of $BaAl_{1.4}Si_{0.6}O_{3.4}N_{0.6}:Eu^{2+}$ concentration: (a) 3000 K; (b) 4000 K; (c) 5000 K

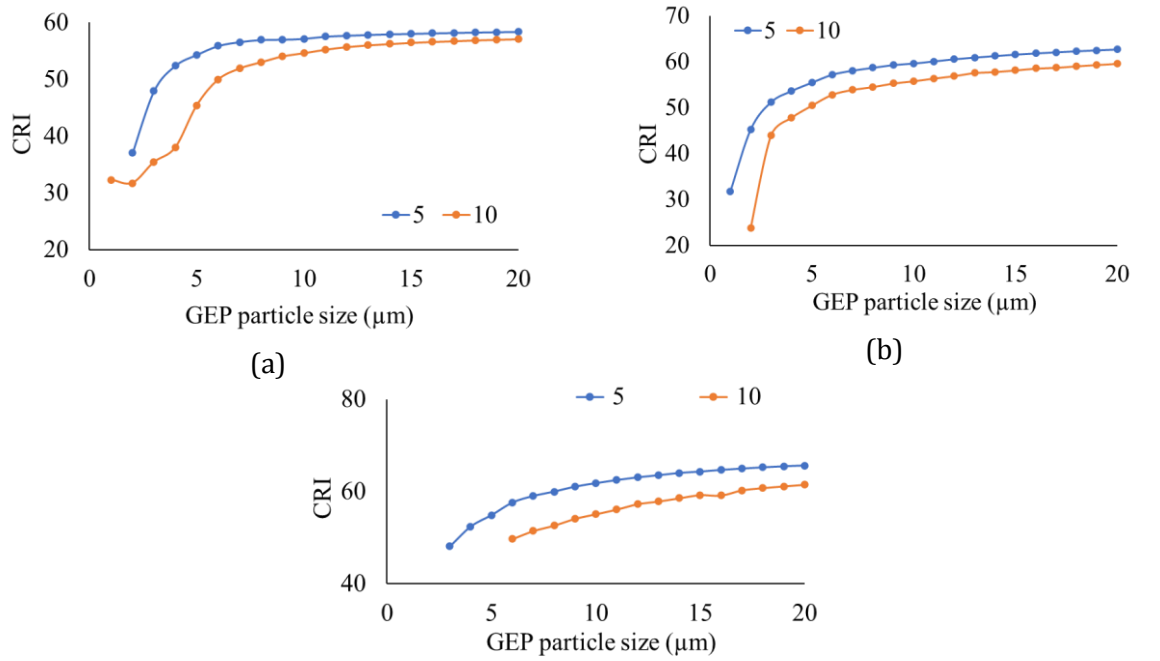

Figure 4 The color rendering index of WLEDs as a function of $BaAl_{1.4}Si_{0.6}O_{3.4}N_{0.6}:Eu^{2+}$ concentration: (a) 3000 K; (b) 4000 K; (c) 5000 K

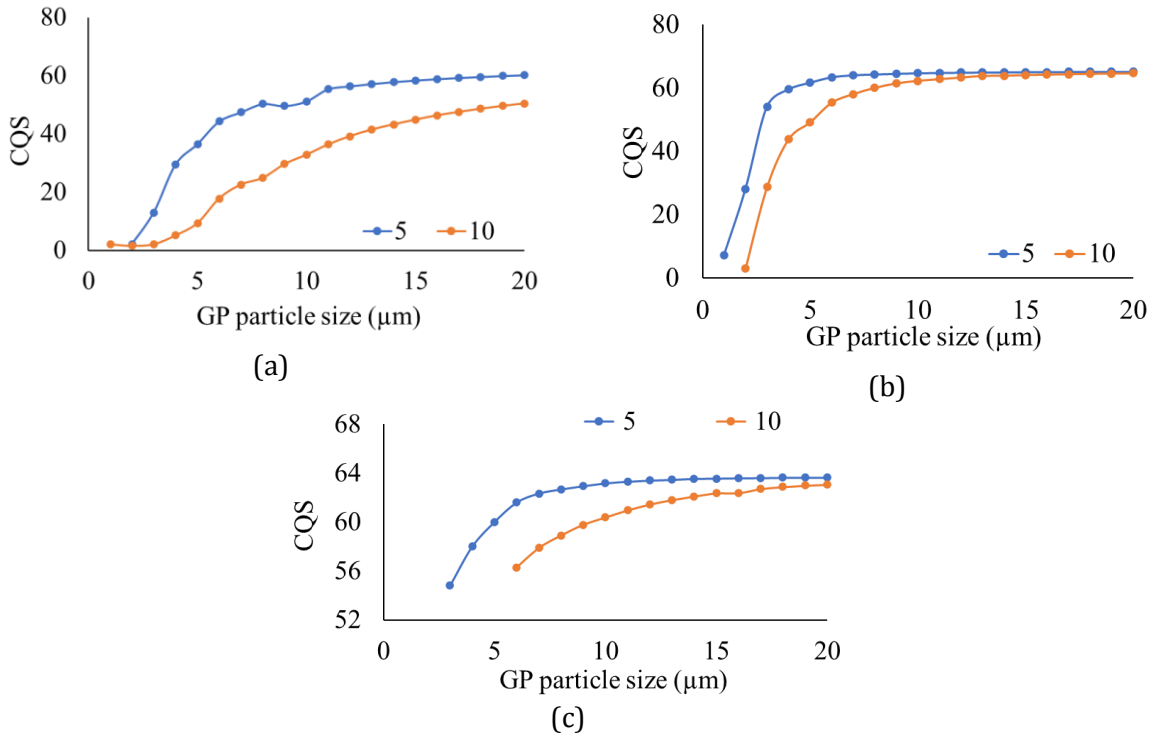

Figure 5 The color quality scale of WLEDs as a function of $BaAl_{1.4}Si_{0.6}O_{3.4}N_{0.6}:Eu^{2+}$ concentration: (a) 3000 K; (b) 4000 K; (c) 5000 K

The addition of GEP $BaAl_{1.4}Si_{0.6}O_{3.4}N_{0.6}:Eu^{2+}$ can help attain sufficient uniformity of white-light chromaticity since it stimulates the blue emission and yellow-green emission spectra. Besides, the scattering losses are incredibly reduced as the low concentration of yellow-emitting YAG:Ce^{3+} is obtained. To investigate the the chromatic feature of white-light generated from pumping blue LED, it is essential to assess the CCT differences for color consistency and color rendering index (CRI) and color quality scale (CQS) for the rendering ability. The attained results for these parameters are demonstrated in Figures 4, 5, and 6, respectively. Overall, the increase in $BaAl_{1.4}Si_{0.6}O_{3.4}N_{0.6}:Eu^{2+}$ concentration is not favourable to the rendering parameters but the color consistency. In particular, the consistency in chromatic is recognized with 10 wt% at 4000 K and 5000 K, see Figures 4 (b) and (c), while 5 wt% could be a better choice for the WLED at 3000 K, see Figures 4 (a). On the other hand, at all CCTs, 10 wt% $BaAl_{1.4}Si_{0.6}O_{3.4}N_{0.6}:Eu^{2+}$ exhibits lower CRI and CQS. With 5 wt% $BaAl_{1.4}Si_{0.6}O_{3.4}N_{0.6}:Eu^{2+}$, it is possible to attain the highest CRI and CQS around 60 at 3000 K and 4000 K CCTs, while at 5000 K CCT, the highest values of these factors can be 65, refer to Figures 5 and 6. This reduction in color rendering factors might be caused by the high proportion of generated green light, which is outstanding over the other light color elements of blue and yellow (Seminara *et al.*, 2021). Besides, the enhanced scattering when increasing phosphor concentration promotes the conversion efficiency yet initiates the imbalance in the color distribution (Sun, You, and Teo, 2022; Khalil *et al.*, 2019). Though the CRI is not as high as expected, the CQS on the other may be sufficient for general lighting. CQS is harder to manage than the CRI, especially at the high CCTs such as 5000 K. This is because the CQS is more complex in assessing elements which include the CRI, the visuality of eyes, and the color coordinate, combining with a larger number of color samples than the original CRI factor (Huu and Thi, 2022). Hence, the color adequacy for in terms of CCT consistency and rendition could be achieved with $BaAl_{1.4}Si_{0.6}O_{3.4}N_{0.6}:Eu^{2+}$. The adjustment of this GEP concentration is recommended depending on the CCT values after taking the luminous requirement into consideration.

4. Conclusions

This work used $BaAl_{1.4}Si_{0.6}O_{3.4}N_{0.6}:Eu^{2+}$ phosphors to enhance the optical factors of the WLED. The phosphor has broad excitation and emission spectra that is suitable for being combined with near-UV or blue-pumping LEDs. The strong emission intensity is recognized in the green spectral wavelength and with a peak observed at 510 nm. The strong intensity of the phosphor might be owing to the accomplished purity and better crystallization when using $NaNO_3$ molten salt as a liquid solvent. The influences of $BaAl_{1.4}Si_{0.6}O_{3.4}N_{0.6}:Eu^{2+}$ on the lighting intensity present that at low CCT of 3000 K, the power strength is improved with low (5wt%) concentration of $BaAl_{1.4}Si_{0.6}O_{3.4}N_{0.6}:Eu^{2+}$. Meanwhile the higher CCTs of 4000 K and 5000 K prefer the higher concentration (10wt%). The color uniformity has the same tendency as the luminous intensity. On the other hand, CRI and CQS are reduced with increasing concentration of $BaAl_{1.4}Si_{0.6}O_{3.4}N_{0.6}:Eu^{2+}$. This may be because of the excessive green light color leading to the light tend to lean over the green region. This is not favourable to color fidelity, which requires balancing color distribution. Therefore, the solution is to use the green phosphor $BaAl_{1.4}Si_{0.6}O_{3.4}N_{0.6}:Eu^{2+}$ with a concentration lower than 10 wt% for better color fidelity.

Acknowledgments

This research is supported by Industrial University of Ho Chi Minh City (IUH) under grant number 121/HD-DHCN.

References

Abeysekera, S.K., Kalavally, V., Ooi, M., Kuang, Y.C., 2020. Impact of circadian tuning on the illuminance and color uniformity of a multichannel luminaire with spatially optimized LED placement. *Optics Express*, Volume 28(1), pp. 130–145

Anh, N.D.Q., Le, P.X. Lee, H., 2019. Selection of a remote phosphor configuration to enhance the color quality of white LEDs. *Current Optics and Photonics*, Volume 3(1), pp. 78–85

Chen, F., Chi, K., Yen, W., Sheu, J., Lee, M. Shi, J., 2019. Investigation on modulation speed of photon-recycling white light-emitting diodes with vertical-conduction structure. *Journal of Lightwave Technology*, Volume 37(4), pp. 1225–1230

David, A., Sahlhoff, D., Wisser, M., 2019. Human perception of light chromaticity: short-wavelength effects in spectra with low circadian stimulation, and broader implications for general LED sources. *Optics Express*, Volume 27, pp. 31553–31566

El-Ghoroury, H.S., Nakajima, Y., Yeh, M., Liang, E., Chuang, C., Chen, J.C., 2020. Color temperature tunable white light based on monolithic color-tunable light emitting diodes. *Optics Express*, Volume 28, pp. 1206–1215

Elkarim, M.A., Aly, M.H., AbdelKader, H.M., Elsherbini, M.M., 2021. LED nonlinearity mitigation in LACO-OFDM optical communications based on adaptive predistortion and postdistortion techniques. Applied Optics, Volume 60(24), pp. 7279–7289

Hao, J., Ke, H., Jing, L., Sun, Q., Sun, R., 2019. Prediction of lifetime by lumen degradation and color shift for LED lamps, in a non-accelerated reliability test over 20,000 h. Applied Optics, Volume 58(7), pp. 1855–1861

Huu, P.D., Thi, D.A.N., 2022. Selection of multi-layer remote phosphor structure for heightened chromaticity and luminous performance of white light-emitting diodes. *International Journal of Technology*, Volume 13(4), pp. 837–847

Ji, J., Zhang, G., Yang, S., Feng, X., Zhang, X., Yang, C.C., 2020. Theoretical analysis of a white-light LED array based on a GaN nanorod structure. *Applied Optics,* Volume 59(8), pp. 2345–2351

Karadza, B., Avermaet, H.V., Mingabudinova, L., Hens, Z., Meuret, Y., 2022. Efficient, high-CRI white LEDs by combining traditional phosphors with cadmium-free InP/ZnSe red quantum dots. *Photonics Research,* Volume 10(1), pp. 155–165

Keshri, S., Marín-Sáez, J., Naydenova, I., Murphy, K., Atencia, J., Chemisana, D., Garner, S., Collados, M.V., Martin, S., 2020. Stacked volume holographic gratings for extending the operational wavelength range in LED and solar applications. *Applied Optics,* Volume 59(8), pp. 2569–257

Khalil, M., Rahmaningsih, G., Gunlazuardi, J., Umar, A., 2019. The influence of plasmonic au nanoparticle integration on the optical bandgap of anatase TiO2 nanoparticles. *International Journal of Technology*, Volume 10(4), pp. 808–817

Le, B., A. White, C.G., Chaudhari, A., AL-Mutawaly, N., White, J.E., Lee, W., Hsu, Y., White, J.D., 2021. Dynamic white lighting to aid sleep and vision for persons living with dementia using off-the-shelf LED strips. *Optics Express,* Volume 29(23), pp. 38606-38614

Li, J., Wu, J., Chen, L., An, X., Yin, J., Wu, Y., Zhu, L., Yi, H., Li, K.H., 2021. On-chip integration of III-nitride flip-chip light-emitting diodes with photodetectors. *Journal of Lightwave Technology*, Volume 39(8), pp. 2603–2608

Ma, Y., Zhang, L., Huang, J., Wang, R., Li, T., Zhou, T., Shi, Z., Li, J., Li, Y., Huang, G., Wang, Z., Selim, F.A., Li, M., Wang, Y., Chen, H., 2021. Broadband emission Gd3Sc2Al3O12:Ce^{3+} transparent ceramics with a high color rendering index for high-power white LEDs/LDs. *Optics Express,* Volume 29(6), pp. 9474–9493

Nahavandi, A.M., Safi, M., Ojaghi, P., Hardeberg, J.Y., 2020. LED primary selection algorithms for simulation of CIE standard illuminants. *Optics Express*, Volume 28(23), pp. 34390–34405

Quesnel, E., Suhm, A., Consonni, M., Reymermier, M., Lorin, G., Laugier, C., Tournaire, M., Le Maitre, P., Lagrange, A., Racine, B., D'Amico, M., Cao, E., 2021. Experimental and theoretical investigation of 2D nanoplatelet-based conversion layers for color LED microdisplays. *Optics Express,* Volume 29(13), pp. 20498–20513

Seminara, M., Meucci, M., Tarani, F., Riminesi, C., Catani, J., 2021. Characterization of a VLC system in real museum scenario using diffusive LED lighting of artworks. *Photonics Research,* Volume 9(4), pp. 548–557

Su, V., Gao, C., 2020. Remote GaN metalens applied to white light-emitting diodes. *Optics Express,* Volume 28(26), pp. 38883–38891

Sun, C.C., You, A.H., Teo, L.L., 2022. XRD Measurement for Particle Size Analysis of PMMA Polymer Electrolytes with SiO_2. *International Journal of Technology*. Volume 13(6), pp. 1336–1343

Wang, L., Wang, X., Kang, J., Yue, C.P., 2021. A 75-Mb/s RGB PAM-4 Visible light communication transceiver system with pre- and post-equalization. *Journal of Lightwave Technology,* Volume 39(5), pp. 1381–1390

Xi, X., Zhang, L., Kang, J., Li, Y., Wang, Z., Fei, B., Cheng, X., Huang, G., Li, M., Chen, H., 2021. Chip-level Ce:GdYAG ceramic phosphors with excellent chromaticity parameters for high-brightness white LED device. *Optics Express,* Volume 29(8), pp. 11938–11946

Xu, S., Hu, H., Shi, Q., Yang, B., Zhao, L., Wang, Q., Wang, W., 2021. Exploration of yellow-emitting phosphors for white LEDs from natural resources. *Applied Optics,* Volume 60(16), pp 4716–4722

Yang, H., Li, P., Ye, Z., Huo, X., Wu, Q., Wang, Y., Wang, Z., 2021. Structural modulation designed a thermally robust blue-cyan emitting phosphor $Y_2Mg_{0.8}Sr_{0.2}$ Al_4Si_{O12}:Eu^{2+} for the high color rendering index white LEDs. *Optics Letters*, Volume 46(22), pp. 5639–5642

Zhang, T., Zhang, X., Ding, B., Shen, J., Hu, Y., Gu, H., 2020. Homo-epitaxial secondary growth of ZnO nanowire arrays for a UV-free warm white light-emitting diode application. *Applied Optics,* Volume 59(8), pp. 2498–2504

Zhong, W., Liu, J., Hua, D., Guo, S., Yan, K., Zhang, C., 2019. White LED light source radar system for multi-wavelength remote sensing measurement of atmospheric aerosols. *Applied Optics,* Volume 58(31), pp. 8542–8548

Zhou, Y., Wei, Y., Hu, F., Hu, J., Zhao, Y., Zhang, J., Jiang, F., Chi, N., 2020. Comparison of nonlinear equalizers for high-speed visible light communication utilizing silicon substrate phosphorescent white LED. *Optics Express,* Volume 28(2), pp. 2302–2316

Zhu, P., Zhu, H., Adhikari, G.C.,Thapa, S., 2019. Spectral optimization of white light from hybrid metal halide perovskites. *OSA Continuum,* Volume 2(6), pp.1880–1888